Journal of Alloys and Compounds 509 (2011) 7410–7415

Contents lists available at ScienceDirect

Journal of Alloys and Compounds

journal homepage: www.elsevier.com/locate/jallcom

Structural, magnetic and magnetocaloric properties of the lanthanum deficient in $La_{0.8}Ca_{0.2-x}\square_xMnO_3$ ($x = 0$–0.20) manganites oxides

M. Khlifi [a], M. Bejar [a], O. EL Sadek [b], E. Dhahri [a,*], M.A. Ahmed [c], E.K. Hlil [d]

[a] Laboratoire de Physique Appliquée, Faculté des Sciences, Université de Sfax, 3000, Sfax, Tunisia
[b] Magnetic and Semiconductor Laboratory, Faculty of Science, Zagazig University, Zagazig,Egypt
[c] Physics Department, Faculty of Science, Cairo University, Giza, Egypt
[d] Institut Néel, CNRS – Université J. Fourier, BP 166, 38042 Grenoble, France

ARTICLE INFO

Article history:
Received 25 February 2011
Received in revised form 6 April 2011
Accepted 9 April 2011
Available online 15 April 2011

Keywords:
Magnetic refrigeration
Calcium-vacancy
Magnetocaloric effect
Rietveld refinement

ABSTRACT

The $La_{0.8}Ca_{0.2-x}\square_xMnO_3$, ($x = 0$–$0.20$) compounds were prepared by the solid-state reaction. X-ray diffraction (XRD) and magnetic measurements were used to investigate the calcium-vacancy effect on the physical properties. The XRD data have been analyzed by Rietveld refinement technique. Samples with $x = 0$, 0.05 and 0.10 are found to be single phase and crystallize in orthorhombic symmetry with *Pnma* space group. Moreover, for $x = 0.15$ and 0.20 samples, the refinement has revealed the coexistence of both *Pnma* orthorhombic and $R\bar{3}c$ rhombohedral phases. The magnetic study has showed that the magnetization exhibits maximum at $x = 0.15$ and minimum at $x = 0.2$. Such behavior was interpreted in terms of orthorhombic distortion contribution, which is related to the orthorhombic structure, leading to magnetization decrease. In addition, maximum magnetic entropy change (ΔS_M) for $x = 0$ sample was found to reach ~4.1 J/kg K under an applied magnetic field of 5 T, which is very sufficient for potential application in magnetic refrigeration. For the same applied magnetic field ($\mu_0 H = 5$ T), the Relative Cooling Power (RCP) values are found to vary between 270 and 300 J/kg. As consequence, the $La_{0.8}Ca_{0.2-x}\square_xMnO_3$ compounds can be used as a composite for magnetic refrigeration in the [175–183] K temperature range.

1. Introduction

Perovskite-type manganites $Ln_{1-x}A_xMnO_3$, where Ln is a rare earth (Ln = La, Pr, Sm . . ..) and A is a divalent element (A = Ca, Sr, Ba, ...), have attracted considerable attention due to their interesting electrical and magnetic properties [1–7]. The interplay between electrical transport and ferromagnetism (FM) in these systems was interpreted by the double-exchange (DE) mechanism [8–10]. This mechanism considers the magnetic coupling between Mn^{3+} and Mn^{4+} ions as resulting from the motion of an electron between two partially filled *d* shells with strong on-site Hund's coupling. For manganites compounds, the existence of the Mn^{3+}–Mn^{4+} mixed valence is necessary to introduce both FM state and metallic conductivity. However, recent studies have shown that the DE interaction alone cannot explain the behaviors observed in these systems. These studies suggest that others effects play a crucial role, such as the charge ordering, the average A-site cation radius $\langle r_A \rangle$ [11–15], the A-site cation size mismatch [14–18], the oxygen deficiency [19–23] and the polarons effect due to the strong electron–phonon interaction arising from the Jahn–Teller distortion [24].

However, only few studies have been proposed to discuss the deficiency effect in manganites system. As known, deficiency in this system leads to a change of Mn^{3+}/Mn^{4+} ratio.

In this paper, we propose to study the effect of vacancies on the structural, magnetic and magnetocaloric properties of $La_{0.8}Ca_{0.2-x}\square_xMnO_3$ ($0 \le x \le 0.20$) compounds.

2. Experimental

Powder samples of $La_{0.8}Ca_{0.2-x}\square_xMnO_3$ ($0.00 \le x \le 0.20$) were prepared using the solid-state reaction, by mixing La_2O_3, CaO and MnO_2 precursors up to 99.9% purity in the desired proportion according to the following reaction:

$$0.4La_2O_3 + (0.2-x)\,CaO + MnO_2 \rightarrow La_{0.8}Ca_{0.2-x}\square_xMnO_3$$

The mixture was initially heated at 973 K to 1373 K during ten days followed by subsequently heating at higher temperature with intermediate grinding. Then, powder was pressed into pellets forms under 4 tones/cm^2 and sintered at 1473 K for 1 day in air with several periods of grinding repelleting. Finally, these pellets were rapidly quenched to room temperature. This step was made in order to keep the structure at the annealed temperature.

The samples structure was characterized by X-ray diffraction with Cu Kα radiation ($\lambda = 1.5406$ Å) by step scanning (0.02°) in the range $20° \le 2\theta \le 100°$. Magnetic measurements were performed in BS2 magnetometer developed in Louis Néel Laboratory of Grenoble. The magnetization curves were obtained under different applied magnetic field with a temperature ranging from 4 to 300 K.

* Corresponding author. Tel.: +216 98373734; fax: +216 74676609.
E-mail address: essebti@yahoo.com (E. Dhahri).

0925-8388/$ – see front matter © 2011 Elsevier B.V. All rights reserved.
doi:10.1016/j.jallcom.2011.04.049

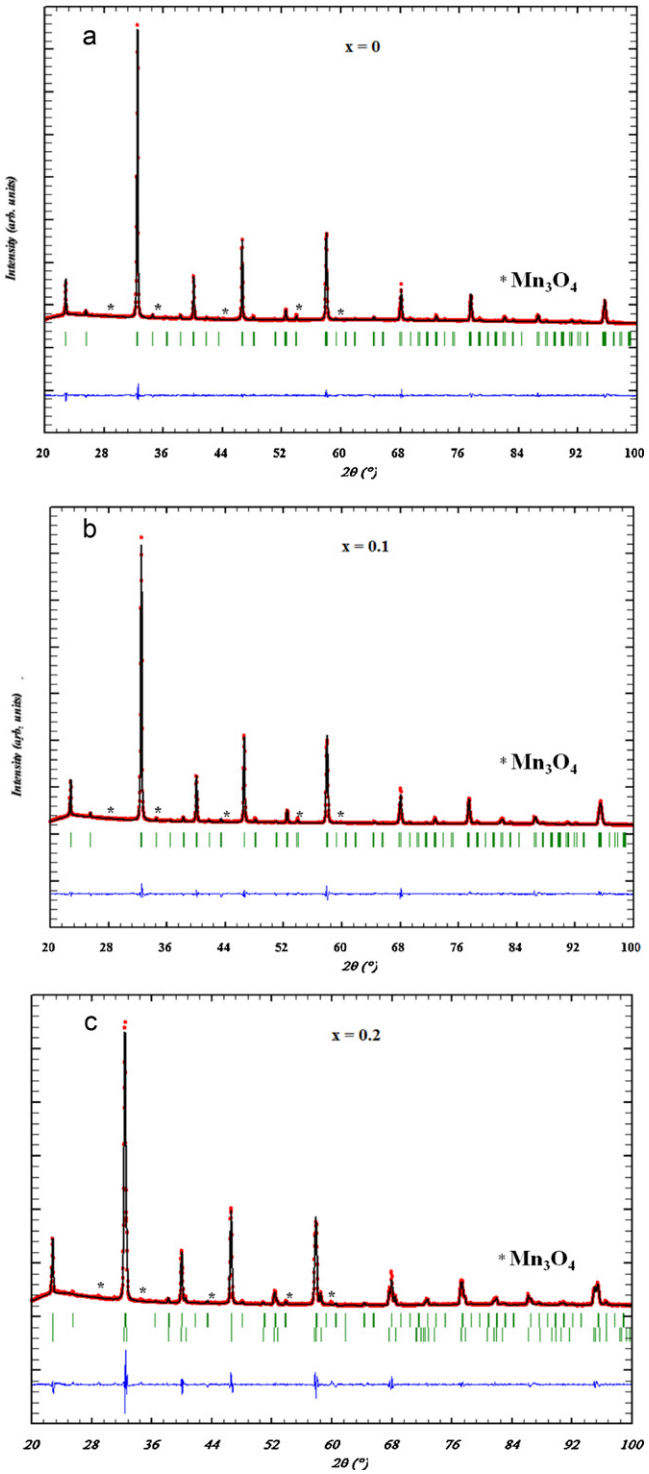

Fig. 1. Observed (circle), calculated (continuous line) and difference patterns (at the bottom) of X-ray diffraction data, for (a) $x = 0$, (b) $x = 0.10$ and (c) $x = 0.20$ of $La_{0.8}Ca_{0.2-x}\square_xMnO_3$ compounds. The vertical tick indicates the allowed reflections.

3. Results and discussion

3.1. X-ray analysis

Phase identification and structural analysis were carried out by X-ray diffraction (XRD) technique with Cu Kα radiation at room temperature. The data were analyzed by the Rietveld method using Fullprof program [25]. Fig. 1 shows examples of the refinement of XRD patterns for $x = 0$, 0.10 and 0.20 samples.

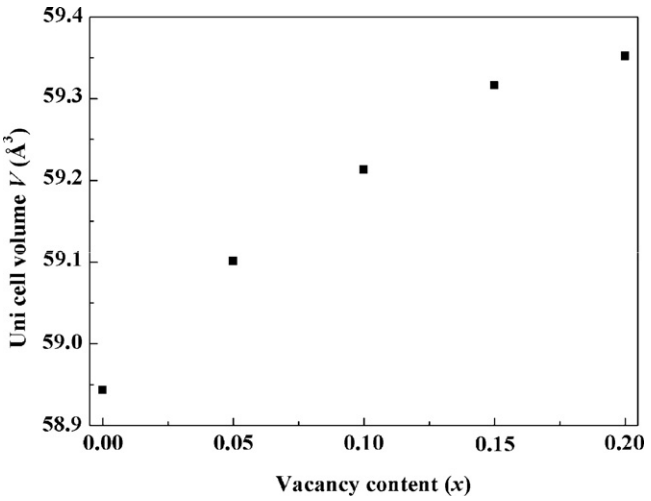

Fig. 2. Variation of the unit cell volume (V) versus the calcium-vacancy content (x) of $La_{0.8}Ca_{0.2x}\square_xMnO_3$ ($0.0 \le x \le 0.20$) compounds.

It was found that samples with $x \le 0.10$ crystallize in the orthorhombic structure with *Pnma* space group. For $x = 0.15$ and 0.20 samples, the refinements have revealed the coexistence of two structures attributed to the *Pnma* orthorhombic and the $R\bar{3}c$ rhombohedral space group. So, we can deduce that, when increasing the vacancy-content (x), there is conversion of a proportion of the orthorhombic structure to the rhombohedral one. This type of conversion is also observed by Pena et al. in the case of $La_{0.7}(Ca_{0.3-x}Cd_x)MnO_3$ compounds [26]. Finally, we note the presence, for all samples, of a secondary phase attributed to the unreacted Mn_3O_4. Related refined cell parameters, unit cell volume, selected interatomic distances and angles are given in Table 1.

In Fig. 2, we have plotted the variation of the unit cell volume (V) versus calcium-vacancy content (x). The $V(x)$ curve reveals an increase of the volume with increasing x.

The introduction of the calcium-vacancy (x) in our samples involves a partial conversion of Mn^{3+} to Mn^{4+} ions according to the formula $La^{3+}_{0.8}Ca^{2+}_{0.2-x}\square_xMn^{3+}_{0.8-2x}Mn^{4+}_{0.2+2x}O^{2-}_3$. The increase of the calcium-vacancy content (x) leads to an augment of Mn tetravalent ion number, which posses a smaller ionic radius ($r_{Mn^{4+}} = 0.53$ Å and $r_{Mn^{3+}} = 0.65$ Å [27]). As result, this leads to a decrease of the B-site radius, which cannot explain the increase of unit cell volume V. As a consequence, there are surely other factors inducing this increase, such as the average ionic radius of the A-site $\langle r_A \rangle$.

For electrostatic considerations, the vacancy has an average radius $\langle r_V \rangle$ non-equal to zero. According to Boujelben et al. [28] in the lacunar (Pr, Sr)MnO_3 perovskite manganites, the vacancy average radius $\langle r_V \rangle$ is smaller than Sr^{2+} ($r_{Sr^{2+}} = 1.31$ Å) and larger than Pr^{3+} ($r_{Pr^{3+}} = 1.179$ Å), hence $1.179\ \text{Å} \le \langle r_V \rangle \le 1.31$ Å.

From this consideration, we can deduce that the $\langle r_V \rangle$ value is also larger than the $r_{Ca^{2+}}$ one (1.18 Å). Therefore, the vacancy content (x) augment results in enhancement of the average radius of the A-site, which can explain the unit cell volume (V) increase.

3.2. Magnetic properties

The stoichiometric sample $La^{3+}_{0.8}Ca^{2+}_{0.2}Mn^{3+}_{0.8}Mn^{4+}_{0.2}O^{2-}_3$ ($x = 0.0$) is ferromagnetic below Curie temperature (T_C). To study the calcium-vacancy effect on the magnetic properties, magnetization variation (M) versus temperature (T) under an applied magnetic field of 0.05 T is measured and reported in Fig. 3. The $M(T)$ curves reveal a ferromagnetic–paramagnetic transition occurring at the Curie temperature (T_C) for all samples when increasing temperature. In addition, the magnetization decreases, when increasing x, for samples with

Table 1
Results of Rietveld refinements, determined from XRD patterns measured at room temperature, for $La_{0.8}Ca_{0.2-x}\square_xMnO_3$ ($0.00 \le x \le 0.20$) compounds.

x	0.00	0.05	0.10	0.15		0.20	
Space group	*Pnma*	*Pnma*	*Pnma*	*Pnma*	$R\bar{3}c$	*Pnma*	$R\bar{3}c$
a (Å)	5.4972	5.5066	5.5050	5.5253	5.5341	5.5120	5.5353
b (Å)	7.7771	7.7937	7.7866	7.8002	5.5341	7.8279	5.5353
c (Å)	5.5149	5.5084	5.5255	5.5152	13.361	5.5124	13.347
Unit cell volume V (Å^3)	58.943	59.101	59.213	59.316		59.332	
$\langle d_{Mn-O} \rangle$ (Å)	1.9796	1.9793	1.9946	1.9860		1.9856	
$\langle \theta_{Mn-O-Mn} \rangle$ (°)	160.280	160.375	157.955	160.671		160.470	

$0 \le x \le 0.10$ and then increases for $x = 0.15$ to decreases finally for $x = 0.20$. The same behavior was observed in our previous work [18]. In this work, we have correlated the physical properties of $La_{0.7}Ca_{0.3-x}K_xMnO_3$ compounds to the effect of disorder resulting from the A-site cation size mismatch. This effect was quantified by both the orthorhombic σ^2(Mn–O) and the local σ^2(A–O) distortions. The first distortion, present only in the orthorhombic structure, leads to the ferromagnetic component lowering.

In the case of $La_{0.8}Ca_{0.2-x}\square_xMnO_3$ compounds presenting an orthorhombic structure ($x \le 0.10$), the increase of x leads to reduction of the double exchange (DE) mechanism between Mn^{3+} and Mn^{4+} ions. This reduction explains the decrease of the magnetization when increasing x. For $x = 0.15$ sample, the appearance of the rhombohedral structure, is accompanied by a partial suppression of the orthorhombic distortion. As consequence, there is an enhancement of the DE mechanism and, as consequence, an increase of the magnetization for this sample ($x = 0.15$).

Finally, for $La_{0.8}\square_{0.2}MnO_3$ sample ($x = 0.20$), the Mn^{3+}/Mn^{4+} ratio is equal to 4/6, for which the double exchange mechanism is dramatically reduced, which can explain the magnetization diminish.

The evolution of dM/dT versus temperature (T) is reported in Fig. 4. Analysis gives evidence of the presence of two peaks. The first one, observed at temperature around 46 K, is ascribed to the existence of the minor ferrimagnetic secondary phase Mn_3O_4 [29,30].

The second main peak is attributed to the ferromagnetic–paramagnetic transition at the Curie temperature (T_C). For $La_{0.8}Ca_{0.2}MnO_3$ ($x = 0$) sample, the T_C value, equal to 183 K, is very close to that found by Hong et al. for the same compound [31]. The variation of the Curie temperature (T_C) versus vacancy-content (x) is represented in Fig. 5. The $T_C(x)$ curve revealed a decrease of T_C when increasing x. This reduction can be explained by the decrease of electron-one bandwidth W given by [32]:

$$\frac{W}{W_0} = \frac{\cos(\pi - \gamma/2)}{\langle d_{Mn-O} \rangle^{3.5}}$$

where γ is the Mn–O–Mn angle, d_{Mn-O} is the Mn–O distance and W_0 a positive constant [32]. The variation of W/W_0 with x is reported in Table 2. In fact, as vacancy has an average radius bigger than Ca^{2+}, the introduction of calcium-vacancy leads to the increase of the average A-site cation radius $\langle r_A \rangle$ as mentioned previously. This increase is accompanied by a more internal pressure generated at the A-site and then the strains at lattice go up. As result, there is more distortion, which explains the appearance of the rhombohedral structure. As consequence, there is less overlap between the Mn3d and O2p orbitals, contributing to a decrease of both electron-one bandwidth W and T_C.

To study the applied magnetic field ($\mu_0 H$) effect on the magnetic properties, a systematic investigation of magnetization with

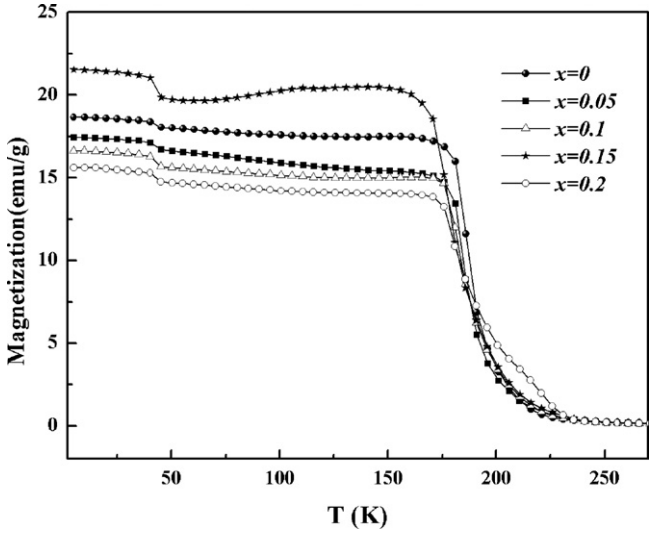

Fig. 3. Variation of the magnetization (M) versus temperature (T) for $La_{0.8}Ca_{0.2-x}\square_xMnO_3$ ($0.0 \le x \le 0.20$) compounds measured at applied magnetic field of 0.05 T.

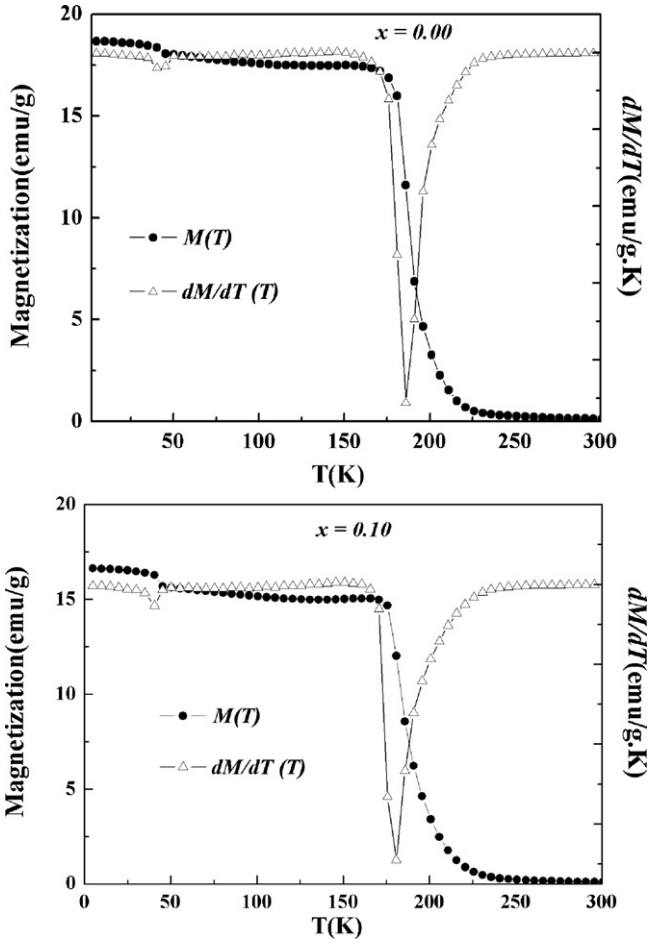

Fig. 4. Variation of the magnetization and the dM/dT as a function of temperature.

Table 2
Nominal vacancies x, bandwidth W/W_0 and Curie temperature T_C.

x	0.00	0.05	0.10	0.15	0.20
W/W_0 ($\times 10^{-2}$)	9.02	9.00	8.92	8. 91	8.79
T_C (K)	183	181	179	177	175

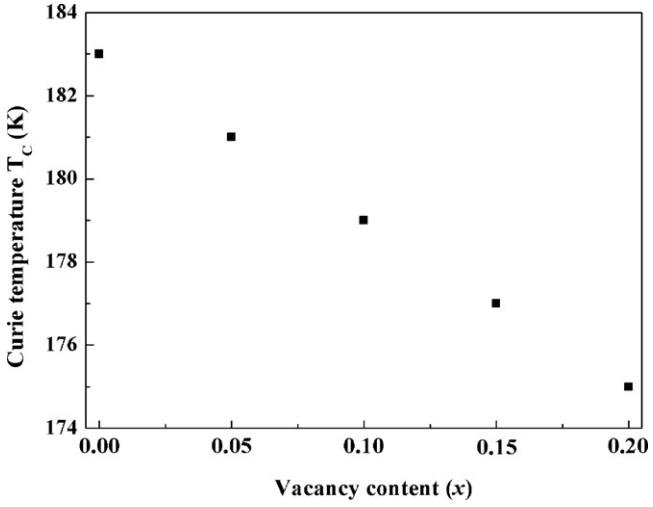

Fig. 5. The calcium-vacancy content (x) dependence of the Curie temperature (T_C).

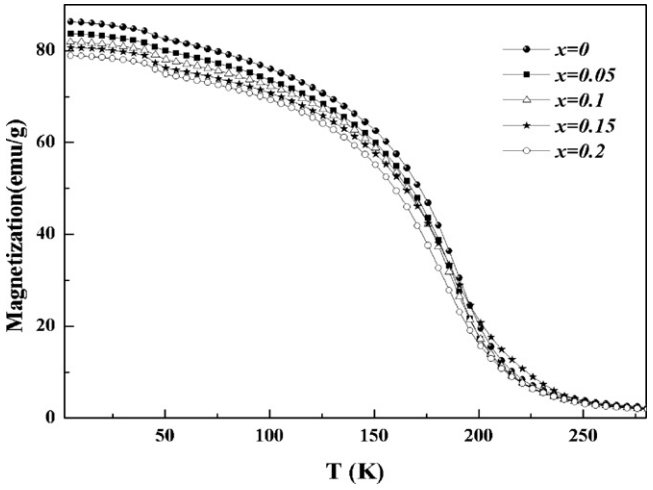

Fig. 6. Temperature dependence of the magnetization of $La_{0.8}Ca_{0.2-x}\square_xMnO_3$ ($0.0 \le x \le 0.20$) compounds for an applied magnetic field of 0.7 T.

temperature has been undertaken at μ_0H value of 0.7 T (Fig. 6). From this figure, we can deduce that the magnetization values determined for $\mu_0H = 0.7$ T are higher than those deduced for an applied magnetic field of 0.05 T. Also, we can conclude, from Fig. 6, that the magnetization decreases linearly with the calcium-vacancy content (x). This difference between the two $M(T)$ curves behaviors (Figs. 3 and 6) can be interpreted in term of suppression of the orthorhombic distortion. In fact, for samples with $x = 0$, 0.05 and 0.10, crystallizing in the orthorhombic structure, the existence of the orthorhombic distortion is accompanied by the presence of an important antiferromagnetic component due to the electron localization. When increasing μ_0H value, there is progressively suppression of this orthorhombic distortion and, as result, reduction of the antiferromagnetic component. Consequently, the electrons are now more delocalized and the double exchange mechanism becomes very important. This delocalization contributes to the increase of magnetization observed for an applied magnetic field of 0.7 T (Fig. 6).

3.3. Magnetocaloric effect

The magnetocaloric effect is an intrinsic property of magnetic materials. It is the response of the material to the application or removal of magnetic field, which is maximized when the material is near its magnetic ordering temperature (Curie temperature T_C).

Fig. 7 shows the magnetic applied field (μ_0H) dependence on the magnetization (M) measured at different temperatures (T) close T_C for $La_{0.8}Ca_{0.2-x}\square_xMnO_3$ compounds.

Based on the thermodynamically theory, the isothermal magnetic entropy change (ΔS_M) associated with a magnetic field variation is given by:

$$\Delta S_M\left(\frac{T_1+T_2}{2}\right) = \frac{1}{T_2-T_1}\left[\int_0^{\mu_0 H_{max}} M(T_2,\ \mu_0 H)\,\mu_0 dH - \int_0^{\mu_0 H_{max}} M(T_1, \mu_0 H)\mu_0 dH\right]$$

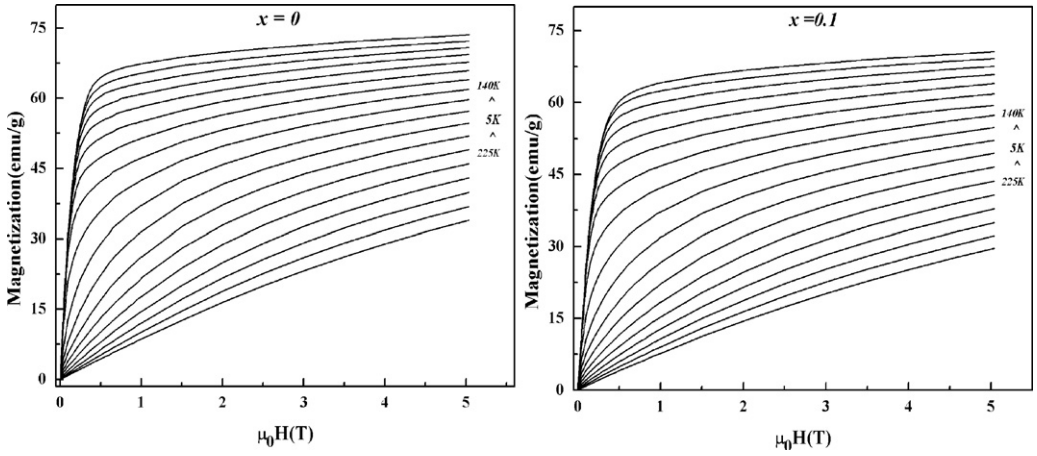

Fig. 7. Isothermal magnetization curves measured at different temperatures around Curie temperature for $La_{0.8}Ca_{0.2-x}\square_xMnO_3$ with $x = 0$ and 0.10.

Table 3
Summary of the Curie temperature, ΔS_{Max} and the RCP values for some magnetocaloric materials.

Material	T_C (K)	ΔS_{Max} (J/K kg)	RCP (J/K)	$\mu_0 \Delta H$ (T)	Reference
$La_{0.8}Ca_{0.2}MnO_3$ (single crystal)	176	3.67	99.09	1.5	[33]
$La_{0.8}Ca_{0.2}MnO_3$ (polycrystalline)	183	2.23	112.36	2	Our work
$La_{0.8}Ca_{0.1}\square_{0.1}MnO_3$ (polycrystalline)	179	2.06	103.72	2	Our work
$Pr_{0.8}Pb_{0.2}MnO_3$	175	2.64	55	1.35	[34]
$La_{0.8}Cd_{0.2}MnO_3$	155	1.01	32	1.35	[35]

Fig. 8 shows the temperature dependence on the magnetic entropy change for different applied magnetic field change interval for $La_{0.8}Ca_{0.2-x}\square_xMnO_3$ compounds with $x = 0$ and 0.1

It can be seen that the magnetic entropy change (ΔS_M) depends on both applied magnetic field and temperature. On the other hand, ΔS_M increases to a maximum value ($\Delta S_{M\,max}$) when the temperature approaches Curie temperature.

The temperature dependence of the $\Delta S_{M\,max}$ value for all calcium-vacancy content (x), upon the magnetic applied field changes of 5 T, is shown in Fig. 9. These curves reveal that all samples present large magnetic entropy change and that $\Delta S_{M\,max}$ decreases when increasing calcium-vacancy content (x). This behavior is understood as the reduction of the double exchange mechanism between Mn^{3+} and Mn^{4+} ions for $La_{0.8}Ca_{0.2-x}\square_xMnO_3$ samples when x increases. Similar behavior is observed for the magnetization measurements performed at applied field of 0.7 T.

The cooling efficiency of magnetic refrigerants is evaluated by means of the so-called relative cooling power RCP corresponding to the amount of heat transferred between the cold and hot sinks in the ideal refrigeration cycle defined as:

$$RCP = -\Delta S_{M\,max} \times \delta T_{FWHM}$$

Where ΔS_{Mmax} is the ΔS maximum and δT_{FWHM} is a full width at half maximum (Fig. 9 inset). We have represented in Fig. 10 the RCP dependence of calcium-vacancy content x at different applied magnetic field. From this curve we can see clearly that the RCP factor remains almost constant for the different x values. For an applied magnetic field of 5 T, the RCP values are found to vary between 270 and 300 J/kg.

While the RCP factor represents a good way for comparing magnetocaloric materials, our compounds can be considered as a potential candidate thanks to their high RCP values comparing with conventional refrigerant materials (Table 3).

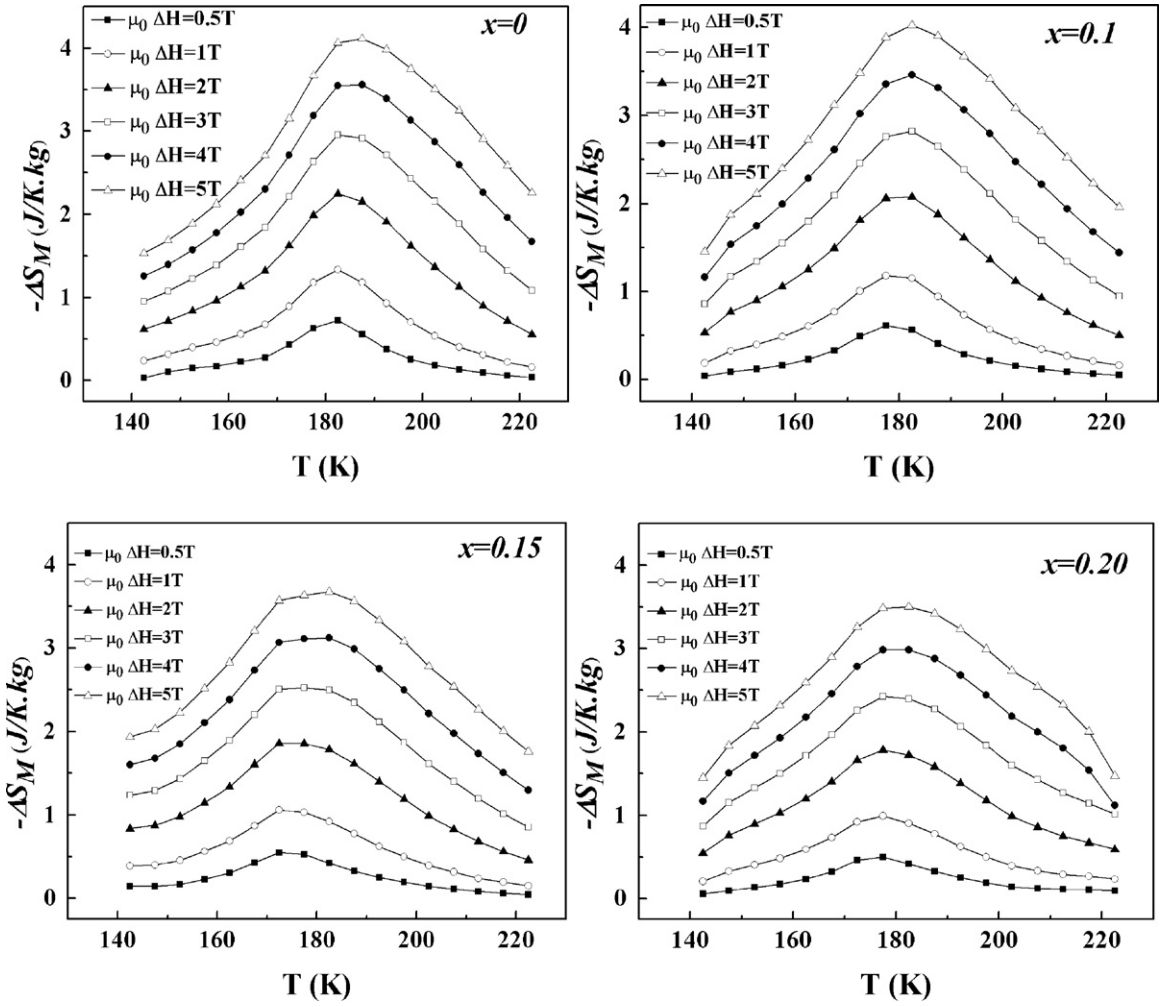

Fig. 8. Temperature dependence of the magnetic entropy change (ΔS_M) at different applied magnetic field change interval for $x = 0$, 0.10, 0.15 and 0.20 samples.

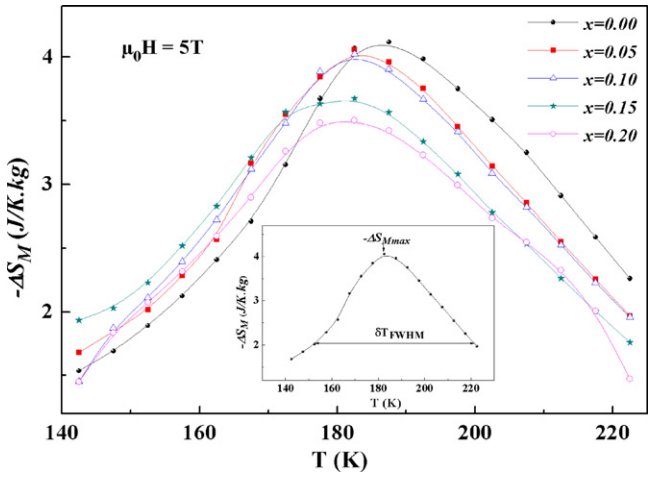

Fig. 9. Temperature dependence of the magnetic entropy change under applied magnetic field of 5 T for $La_{0.8}Ca_{0.2-x}\square_xMnO_3$ ($0.0 \le x \le 0.20$) compounds.

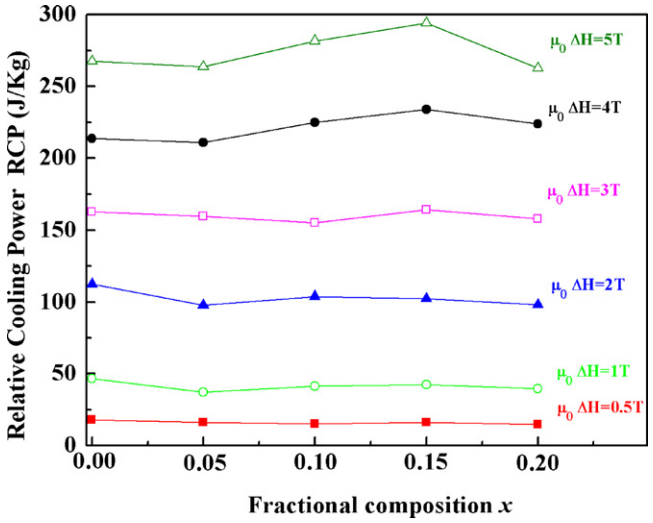

Fig. 10. Variation of RCP factor as function of calcium-vacancy content (x).

On the other hand, a refrigerator able to work in a broad temperature range can be made of a series of magnetocaloric materials with important and comparable RCP factor. These materials are combined in order to form a composite refrigerant working in the temperature range limited by their T_C. This condition is satisfied for $La_{0.8}Ca_{0.2-x}\square_xMnO_3$ compounds, which seem to be advantageous for magnetic refrigeration cycle over the temperature range 183–175 K, because of their interesting RCP factor and the fact that T_C can be tuned easily by changing the vacancy-content (x).

4. Conclusion

The calcium-vacancy effect on the structural, magnetic and magnetocaloric properties of $La_{0.8}Ca_{0.2-x}\square_xMnO_3$ compounds was investigated. The structural study has revealed the presence of a *Pnma* orthorhombic structure for samples with $x \le 0.10$. For $x = 0.15$ and 0.20 samples, the Rietveld refinement pointed out to the coexistence of both *Pnma* orthorhombic and the $R\bar{3}c$ rhombohedral structures. The appearance of the rhombohedral structure was found to modify the magnetic properties. In fact, the increase of the vacancy-content x induces a partial suppression of the orthorhombic structure and, hence a reduction of the orthorhombic distortion. Such reduction was found to be accompanied by more delocalized electrons and, as consequence, an enhancement of both double exchange mechanism and magnetization. From the magnetocaloric results, we have deduced that our compounds present a large magnetic entropy change and can be used like a magnetic refrigerant.

Finally, the $La_{0.8}Ca_{0.2-x}\square_xMnO_3$ compounds can be considered as a good candidate to be used as a composite for magnetic refrigeration in the [175–183] K temperature range due to their interesting RCP factor.

Acknowledgements

This work, within the framework of collaboration, is supported by:

- The Tunisian Ministry of Higher Education and Scientific Research.
- The Egyptian Ministry of High Education.
- The French Ministry of Higher Education and Scientific Research.

References

[1] R. Von Helmolt, J. Wecker, B. Holzapfel, L. Schultz, K. Samwer, Phys. Rev. Lett. 71 (1993) 2331.
[2] R.D. Sanchez, J. Rivas, C.V. Vazquez, A.L. Quintela, M.T. Causa, M. Tovar, S. Oseroff, Appl. Phys. Lett. 68 (1996) 134.
[3] W. Zhang, I.W. Boyd, N.S. Cohen, Q.T. Quentin, A. Pankhaurst, Appl. Surf. Sci. 109 (1997) 350.
[4] F. Damay, C. Martin, M. Hervieu, A. Maignan, B. Raveau, G. Andre, F. Bouree, J. Magn. Magn. Mater. 184 (1998) 71.
[5] A. Peles, H.P. Kunkel, X.Z. Zhou, G. Williams, J. Phys.: Condens. Matter 11 (1999) 8111.
[6] C. Martin, A. Maignan, M. Hervieu, B. Raveau, Phys. Rev. B 60 (1999) 12191.
[7] S. Othmani, M. Bejar, E. Dhahri, E.K. Hlil, J. Alloys Compd. 475 (2009) 46–50.
[8] C. Zener, Phys. Rev. 82 (1951) 403.
[9] P.W. Anderson, H. Hasegawa, Phys. Rev. 100 (1955) 675.
[10] P.G. de Gennes, Phys. Rev. 118 (1960) 141.
[11] R. Mahesh, R. Mahendiran, A.K. Raychaudhuri, C.N.R. Rao, J. Solid State Chem. 114 (1995) 297.
[12] F. Damay, C. Martin, A. Martin, B. Raveau, J. Appl. Phys. 81 (1997) 1372.
[13] N. Abdelmoula, E. Dhahri, K. Guidara, J.C. Joubert, Phase Transitions 69 (1999) 215.
[14] N. Abdelmoula, E. Dhahri, N. Fourati, L. Reversat, J. Alloys Compd. 365 (2004) 25–30.
[15] M. Bejar, H. Feki, E. Dhahri, M. Ellouze, M. Balli, E.K. Hlil, J. Magn. Magn. Mater. 316 (2007) e707–e709.
[16] L.M. Rodriguez-Martinez, J.P. Attfield, Phys. Rev. B 54 (1996) 15622.
[17] F. Damay, C. Martin, A. Maignan, B. Raveau, J. Appl. Phys. 82 (1997) 6181.
[18] M. Bejar, E. Dhahri, E.K. Hlil, S. Heniti, J. Alloys Compd. 440 (2007) 36–42.
[19] A.K.M. Akther Hossain, L.F. Cohen, T. Kodenkandeth, J. Mac-Manus-Driscoll, N.M. Alford, J. Magn. Magn. Mater. 195 (1999) 31.
[20] I.O. Troyanchuk, S.V. Trukhanov, H. Szymezak, K. Baerner, J. Phys.: Condens. Matter 12 (2000) L155.
[21] N. Abdelmoula, K. Guidara, A. Cheikhrouhou, E. Dhahri, J.C. Joubert, J. Solid-State Chem. 151 (2000) 139.
[22] N. Sdiri, M. Bejar, M. Hussein, S. Mazen, E. Dhahri, J. Magn. Magn. Mater. 316 (2007) 703–706.
[23] N. Sdiri, M. Bejar, E. Dhahri, J. Magn. Magn. Mater. 311 (2007) 512–516.
[24] A.J. Millis, P.B. Littlewood, B.I. Shraiman, Phys. Rev. Lett. 74 (1995) 5144.
[25] R.A. Young, The Rietveld Method, Oxford University Press, New York, 1993.
[26] A. Pena, J. Gutierrez, J.M. Barandiaran, J.P. Chapman, M. Insausti, T. Rojo, J. Solid State Chem. 174 (2003) 52–59.
[27] R.D. Shannon, Acta Crystallogr. Sect. A 32 (1976) 751.
[28] W. Boujelben, A. Cheikh-Rouhou, J. Pierre, J.C. Joubert, Physica B 321 (2002) 37–44.
[29] S. Zemni, A. Gasmi, M. Boudard, M. Oumezzine, Mater. Sci. Eng. B 144 (2007) 117–122.
[30] R. Regmi, R. Tackett, G. Lawes, J. Magn. Magn. Mater. 321 (2009) 2296–2299.
[31] C.S. Hong, et al., Phys. Rev. B 63 (2001) 092554.
[32] P.G. Radaelli, G. Iannone, M. Marezio, H.Y. Hwang, S.-W. Cheong, J.D. Jorgensen, D.N. Argyriou, Phys. Rev. B 56 (1997) 8265–8276.
[33] M.H. Phan, V.T. Phan, S.C. Yu, J.R. Rhee, N.H. Hur, J. Magn. Magn. Mater. 272–276 (2004) 2338.
[34] M.H. Phan, H.X. Peng, S.C. Yu, D.T. Hanh, N.D. Tho, N. Chau, J. Appl. Phys. 99 (2006) 08Q108.
[35] K.A. Gschneidner, V.K. Pecharsky, Annu. Rev. Mater. Sci. 30 (2000) 387.